Presented at the 1991 ASME Winter Annual Meeting
Dec. 2-6, 1991

Analysis of Milling Forces via Angular Convolution

J.-J. Junz Wang, Research Assistant
Steven Y. Liang, Assistant Professor
Wayne J. Book, Professor
George W. Woodruff School of Mechanical Engineering
Georgia Institute of Technology
Atlanta, GA 30332-0405

Abstract

The measurement of cutting force systems is one of the most frequently used techniques for the monitoring of machining processes. Its wide spread application ranges from tool condition identification, feedback control, cutting system design, to process optimization. To gain fundamental understanding of the force system in machining, this paper presents the work of establishing a closed form expression for the cutting force in end milling as an explicit function of cutting parameters and tool/workpiece geometry. Based on the theoretical local cutting force model, the generation of total cutting forces is formulated as the angular convolution of three uncorrelated cutting process component functions, namely the elemental cutting force function, the chip width density function, and the tooth sequence function. The elemental cutting force function is related to the chip formation process in an elemental cutting area and it is characterized by the chip thickness variation, specific cutting pressure constants, and entry/exit angles. The chip width density function defines the chip width per unit cutter rotation along a cutter flute within the range of axial depth of cut as the function of the angular position of each cutting point. The tooth sequence function represents the spacing between flutes as well as their cutting sequence as the cutter rotates. The analysis of cutting forces is extended into the Fourier domain by taking the frequency multiplication of the transforms of the three component functions. Fourier series coefficients of the cutting forces are shown to be algebraic functions of various tool parameters and cutting conditions. Simulation results are presented in the frequency domain to illustrate the effects of process parameters. A series of end milling experiments are performed and their results discussed to validate the analytical model.

1. Introduction

The measurement of cutting forces is one of the most frequently used techniques for machining process monitoring because the cutting forces are closely related to part dimensional accuracy, surface finish, tool condition, chip morphology, and machining stability. The fundamental understanding of the cutting force systems thus plays an important part in the monitoring, planning, and control of machining processes as well as in its traditional role in the design of machine tool structure and axes servomechanisms. Research in this area dates back to the work of Martellotti [1941, 1945] on the

kinematics of the milling process. The basic cutter-chip thickness relationship took the form of

$$t_c = t_x \sin\theta \tag{1}$$

where t_c is the instantaneous undeformed chip thickness, t_x is the feed per tooth in the feed direction and θ is the angular position of the tooth in the cut as seen in Figure 1. In this expression, the tooth trajectory of a milling cutter was assumed to be circular instead of cycloidal, therefore the equation is not an exact solution for the chip thickness, however it is a good approximation when the feed is much less than the cutter diameter, and it has been widely used in the analysis of the milling process. The relation indicated that the cutting force generated by a certain chip thickness depends upon tool edge geometry such as clearance and rake angles as well as properties of the tool and workpiece material.

Simple models have been proposed [Koenigsberger et al. 1961, Sabberwal 1962] to relate the tangential cutting force (f_t) at any location on the cutting edge to the chip thickness in the following form:

$$f_t = K_t b t_x \sin\theta \tag{2}$$

where b is the width of chip and K_t is the tangential specific cutting pressure constant, which is a function of tool edge geometry and workpiece material properties and is usually evaluated from experiments. It has been shown that K_t is a function of the chip thickness and, for simplicity, its value corresponding to the average chip thickness has been commonly used since the average chip thickness can be easily calculated from the average cutting force.

Based on the local cutting force model, total cutting force models for the milling process were derived by incorporating the considerations of cutting conditions, cutter geometry, feedrate, and axial and radial depth of cut. Closed form integration expressions for the total cutting force on a given flute have been established as a function of the cutter angular position [Koenigsberger et al. 1961, Tlusty et al. 1975]. Using integration models, Koenigsberger and Sabberwal investigated the force pulsation during the milling process and developed quantitative force relationships for slab and face millings. These relationships showed the magnitude of the average force and the ratio of maximum to average forces for different dimensions and positions of the cutter relative to the workpiece. In addition to equation (2), Tlusty and MacNeil related the tangential cutting force (f_t) to the the radial cutting force (f_r) by the radial specific cutting pressure K_r:

$$f_r = K_r f_t \tag{3}$$

and developed the cutting dynamics in end milling. It was experimentally observed that the cutting force responding to a sudden feedrate change can often be characterized by a time delay, which may give rise to instability in adaptive control. These cutting force models were given in terms of the cutter angular position and different expressions were needed to evaluate forces at different angular positions. Therefore the integration solutions were segmented into different formulations with different integration boundary points.

Most of the integration expressions of the cutting force system applied to one cutter flute only. For a multi-flute cutter, care has to be taken to determine which flutes are engaged in the cutting and which appropriate integration form is to be used. Gygax conducted a detailed analysis [1979] and a series of experiments [1980] on the dynamics of single-tooth face milling under various cutting parameters. It was indicated that the extension of single-tooth milling to multi-tooth face milling could be achieved by convolution integration in the time domain. This was the first appearance of the convolution modeling concept in the literature. However, no cutting force modeling technique was

presented and more complicated end millings were not treated.

Resorting to numerical integration, Kline, DeVor and Lindberg [1982, 1983] developed mechanistic discrete models for end milling in which the cutter is treated as an aggregation of discretized thin disk cutters along the cutter axis. At any angular position, chip load of each disk cutter can be computed as the product of chip thickness and disk thickness. The associated cutting forces can then be found from equations (2) and (3). Summation of forces from all disks yields the total cutting forces. Sutherland and DeVor [1986] improved on the previous model by taking into account the effects of system deflection on the chip load. Following from Kline's model, Fu, DeVor, and Kapoor [1984] developed a cutting force model for face milling which included the effects of spindle tilt and cutter runout. Alternatives to treat the elemental cutting forces differently were reported in the works of Zhou [1983], Ber [1988] and Armarego [1989], however, these formulations still rely on numerical integration to compute the total milling forces.

Up to now there is no documented technique to model the complete cutting force system of milling processes in a single closed form representation. The fact that the existing cutting force models are either inappropriate for multi-flute cutting or rely upon numerical integration for solutions leads to the difficulties in interpreting the cutting force measurements. Therefore their applications in cutting dynamic analysis and process optimization are restricted. On the other hand, there is a lack of milling force model in the frequency domain or transfer function representation. As a result, some of the adaptive control schemes with cutting force as the control constraint had to resort to the parameter identification based on assumed process models [Tomizuka et al. 1983, Lauderbaugh et al. 1988, Fussel et al. 1988]. However, uncertainties in the assumed model structure often raised stability concerns [Rohrs et al. 1985] and limited the scope of milling process controls.

This paper presents the work of establishing a closed form frequency domain expression for the cutting force in end milling as an explicit function of cutting parameters and tool/workpiece geometry through angular convolution modeling. The angular domain analysis is discussed in section 2. The frequency domain formulation along with numerical results are presented in section 3. Section 4 provides the description of experiments and the discussion of analytical model validation based on experimental results.

2. Convolution modeling of Multi-tooth Milling Forces

In the following analysis the complete cutting force system at any instance of cutting is considered as the time-domain convolution of the cutting forces on any elemental point on the cutter, the width of chip produced during unit angular rotation of the cutter, and an impulse train representing the sequence of tooth engagement. These three components of the time-domain convolution can be written as functions of cutter angular position thus the convolution integral can be carried out in the angular domain. The derivation of these components, namely the elemental cutting force function, the chip width density function, and the tooth sequence function, is discussed in detail in this section. Attention will be directed to the cases of ideal cutting in which cutting speed and feedrate are both constant while cutter runout and tilt do not exist, although deviations from ideal cases can be treated as well.

2.1 Elemental Cutting Force Functions

The analysis begins with considering a differential cutting point on any flute of a multi-tooth cutter. As the cutter rotates, the cutting point experiences a pattern of cutting forces as functions of the cutter angular position with respect to the workpiece. These force functions are described in equations (2) and (3), which can be expressed in X and Y coordinates as follows:

$$f_x(\theta) = f_t \cos\theta + f_r \sin\theta \qquad (4)$$

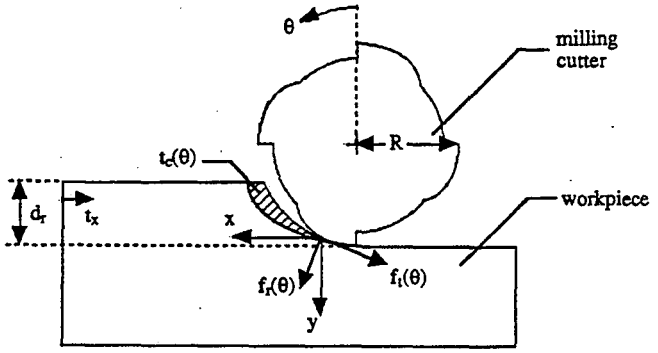

Figure 1. Geometric relationship between undeformed chip thickness (t_c), feed per tooth (t_x), and cutting forces ($f_t(\theta)$, $f_r(\theta)$).

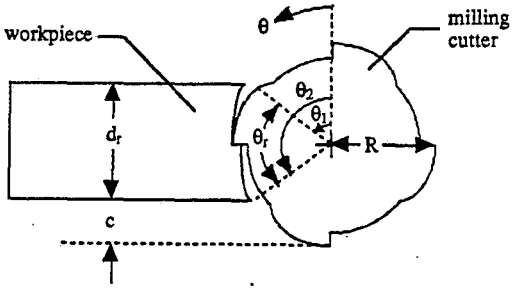

Figure 2. Entry angle (θ_1)and Exit angle (θ_2)of a milling cutter.

$$f_y(\theta) = f_t \sin\theta - f_r \cos\theta \tag{5}$$

Notice that the cutting force expressions in (4) and (5) are applicable only over the range of cutter angular position during cutter-work engagement. This range of angular position is the difference between the cutter entry angle θ_1 and the cutter exit angle θ_2 as shown in figure 2. Denoting the radius of cutter by R, radial depth of cut by d_r, and cutter width excess by c in the figure,

$$\theta_1 = \cos^{-1}\left(\frac{d_r + c}{R} - 1\right) \tag{6}$$

$$\theta_2 = \cos^{-1}\left(\frac{c}{R} - 1\right) \tag{7}$$

By defining a window function $w(\theta)$ as follows

$$w(\theta) = \begin{cases} 1, & \theta_1 \le \theta \le \theta_2 \\ 0, & \text{otherwise} \end{cases} \tag{8}$$

cutting forces in equations (4) and (5) can be expressed in more precise terms as

$$\begin{bmatrix} f_x(\theta) \\ f_y(\theta) \end{bmatrix} = \begin{bmatrix} \cos\theta & \sin\theta \\ \sin\theta & -\cos\theta \end{bmatrix} \begin{bmatrix} f_t(\theta) \\ f_r(\theta) \end{bmatrix} w(\theta) \tag{9}$$

The position and width of the window function are determined by the type of milling process and its cutting conditions. For a peripheral milling, the window depends on the cutter radius and the width of cut, and it generally starts at an angle greater than 90 degrees and ends at 180 degrees for down milling. For a slot milling, it starts at 0 and ends at 180 degrees.

The elemental cutting force functions, p_x and p_y, are defined as the forces acting on an elemental cutting area per unit specific cutting pressure (K_t). That is

$$p_x(\theta) = \frac{f_x(\theta)}{K_t\, b\, t_x} \tag{10}$$

$$p_y(\theta) = \frac{f_y(\theta)}{K_t\, b\, t_x} \tag{11}$$

From equations (4), (5), (9)-(11), it can be shown that

$$\begin{bmatrix} p_x(\theta) \\ p_y(\theta) \end{bmatrix} = \begin{bmatrix} 1 & K_r \\ -K_r & 1 \end{bmatrix} \begin{bmatrix} p_1(\theta) \\ p_2(\theta) \end{bmatrix} \tag{12}$$

where

$$p_1(\theta) = \frac{\sin 2\theta}{2}\, w(\theta) \tag{13}$$

$$p_2(\theta) = \frac{1-\cos 2\theta}{2}\, w(\theta) \tag{14}$$

which are graphically depicted in Figure 3.

The elemental cutting force functions are the same for all cutting points anywhere on the cutter since they are defined with respect to a unit cutting area. The contributions of different cutting points on a flute to the total cutting forces differ only in the cutter angular position in which they engage in the cutting. Since points on a flute engage in the cutting in a predetermined sequence as dictated by the cutter geometry, these points produce orderly shifted functions of the same elemental cutting forces. The superposition of these shifted force functions sums to the total cutting forces. Thus, we can treat the elemental cutting process as a linear shift-invariant system and think of the force functions generated at an elemental cutter point, namely p_x and p_y, as finite cutting impulse response functions of duration θ_r.

2-2 Chip Width Density Function

The elemental cutting forces are defined with respect to a unit width of cut while the chip width density function, cwd(θ), discussed herein is the chip width produced during unit angular rotation of the cutter; therefore the chip width density function can be used to weigh each elemental force within the range of the axial depth of cut. In general, for constant or variable helix angle cutters, the chip width density function is determined from

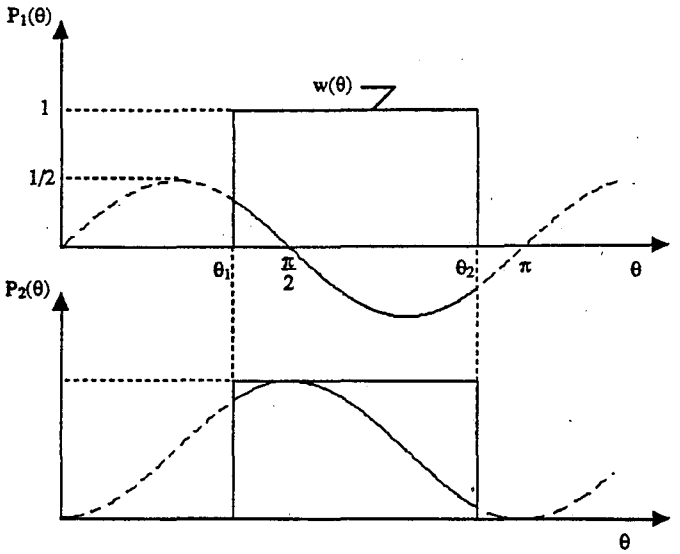

Figure 3. Functions $P_1(\theta)$ and $P_2(\theta)$ in the expression of elemental cutting forces.

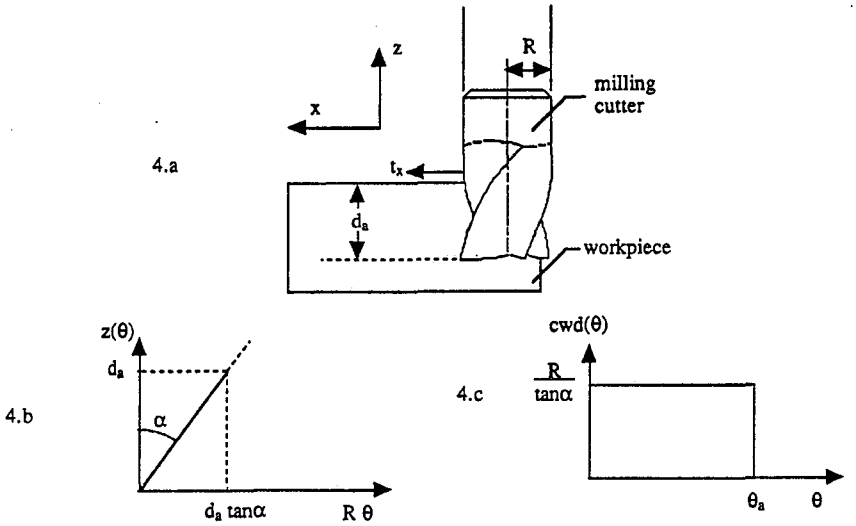

Figure 4. Relationship between the axial depth of cut and chip width density function.

$$cwd(\theta) = \frac{dz(\theta)}{d\theta} \tag{15}$$

where $z(\theta)$ is the axial position of a point along the cutter flute as a function of the angular position of that point. Shown in Figure 4.b is an unfolded flute, with helix angle α, bounded by the axial depth of cut d_a. Its chip width density function is

$$cwd(\theta) = \frac{R}{\tan\alpha} \qquad 0 \le \theta \le \frac{d_a \tan\alpha}{R} \tag{16}$$

which is a rectangular pulse function as shown in Fig 4.c. Notice that the total area of the rectangular pulse has a value equivalent to the axial depth of cut. For cutters with a smaller helix angle, the width and height of their chip width density functions are smaller and greater respectively. In the extreme case of a straight teeth cutter (α=0), the function degenerates to an impulse function with an area of d_a.

The chip width density function derived above is applicable to any flute on the cutter. As the milling cutter rotates, each flute will contribute to the total cutting force system through the same chip width density function except that the function is shifted by an angle equivalent to the spacing between flutes. Therefore, the chip width density representation can again be treated as a shift-invariant process with the chip width density function being the impulse response weighed by a tooth sequence function, which represents the continuous cutter rotation and the angular spacing between cutter flutes.

2-3 Tooth Sequence Function

For a cutter with evenly spaced flutes, the tooth sequence function ts(θ) can be determined from

$$ts(\theta) = t_x \sum_{k=0}^{\infty} \delta(\theta - \frac{2\pi}{n} k) \tag{17}$$

where n is the number of flutes on the cutter and δ is the unit impulse function. The function is essentially a train of impulses separated by $\theta_p = \frac{2\pi}{n}$, the angular spacing between any two neighboring flutes.

2-4. Total Cutting Force

The total cutting forces, $\bar{f}_x$ and $\bar{f}_y$, are the angular domain convolution of the elemental cutting force function, the chip width density function, and the tooth sequence function. Denoting convolution operation by "*", cutting forces are expressed as:

$$\begin{bmatrix} \bar{f}_x(\theta) \\ \bar{f}_y(\theta) \end{bmatrix} = K_t\, ts(\theta) * cwd(\theta) * \begin{bmatrix} p_x(\theta) \\ p_y(\theta) \end{bmatrix} \tag{18}$$

Defining the angular convolution of the tooth sequence function and the chip load function as inp(θ), it can be shown that

$$\begin{aligned} inp(\theta) &= ts(\theta) * cwd(\theta) \\ &= \int_0^{\theta} ts(\tau)\, cwd(\theta-\tau)\, d\tau \\ &= \int_0^{\theta} t_x \sum_{k=0}^{\infty} \delta(\tau - \frac{2\pi}{n} k)\, cwd(\theta-\tau)\, d\tau \\ &= t_x \sum_{k=0}^{\infty} cwd\,(\theta - \frac{2\pi}{n} k) \end{aligned} \tag{19}$$

which is a periodic function with an angular period of θ_p as shown in Figure 5.

It follows from equations (18) and (19) that

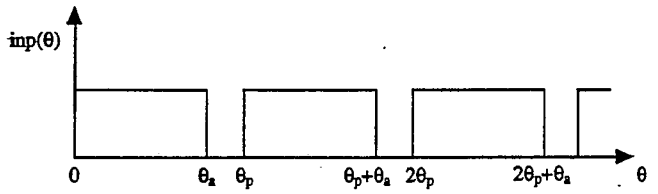

Figure 5. The angular convolution of the tooth sequence function and the chip load function.

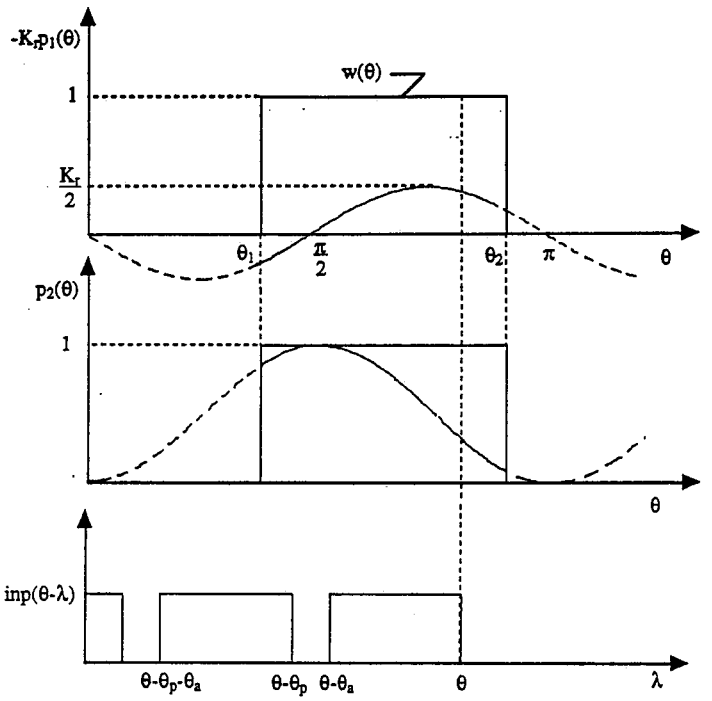

Figure 6. Angular convolution model of total cutting force in y direction.

$$\begin{bmatrix} \bar{f}_x(\theta) \\ \bar{f}_y(\theta) \end{bmatrix} = K_t\, inp(\theta) * \begin{bmatrix} p_x(\theta) \\ p_y(\theta) \end{bmatrix} = K_t\, t_x \int_0^{\theta} \sum_{k=0}^{\infty} cwd(\theta - \tau + \frac{2\pi}{n}k) \begin{bmatrix} p_x(\tau) \\ p_y(\tau) \end{bmatrix} d\tau \qquad (20)$$

This is an unified expression for the milling force system in the angular domain. The convolution integral provides a clear insight into the effects of cutting parameters on the milling process. To illustrate this point, a graphical representation of the convolution process for the y component of the cutting force is given in Figure 6. In the convolution integral, the function inp(θ) is rotated with respect to the ordinate and shifted toward the right side. The y cutting force is the area under a function defined as the product of the elemental cutting force $p_y(\theta)$, the rotated and shifted inp(θ), and the specific cutting pressure K_t. Since $p_y(\theta)$ is bounded by the window function w(θ), the cutting force is equivalent to the total area of the product function within the window. As the cutter rotates, the function inp(θ-λ) moves toward right and the total cutting force will experience a periodic variation

with a period of θ_p. Three phases of cutting as discussed in [Tlusty et al., 1975] can be clearly visualized as the first cutting edge of the flute enters the window, stays in it, and exit from it. In addition, several comments can be made from the convolution expression regarding the effects of θ_a, θ_p, and θ_r (defined as θ_2-θ_1 as shown in Figure 2) on the characteristics of total cutting forces:

1. If the axial depth of cut (d_a) and the angle of circumferential engagement (θ_r) are both small such that the gap in the inp(θ) is greater than the width of the window function, that is, θ_p-θ_a>θ_r, there will be zero cutting force for a duration of θ_p-θ_a-θ_r. In this case, at most one flute is engaged in the cutting at any instant of time.

2. If the axial depth of cut and the angle of circumferential engagement are both large such that θ_p-θ_a<θ_r, at least two flutes are engaged in cutting for a duration of θ_r-θ_p+θ_a.

3. If θ_a is identical to θ_p, one flute engagement will be immediately followed by the engagement of another. The function inp(θ) in this case becomes a DC function independent on time. As a result, cutting force system will assume a constant value at steady state cutting.

4. If the angle of axial engagement (θ_a) is greater than the angular tooth spacing (θ_p), cutting edges will overlap in time. The cutting force system in this situation can be described by that in the previous case superimposed by that in a case with axial engagement angle equals to θ_a-θ_p.

5. The areas under p_x and p_y versus θ curve within the window is an indication of the average cutting force. By appropriate positioning of the cutting window, zero average cutting force could be obtained.

3. Frequency Domain Model

The frequency characteristics of cutting forces can be studied by examining the three model functions in the Fourier domain. In the following discussion, the transforms of these functions from the angular domain to the spectral domain is performed while the frequency variables are normalized with respect to the spindle rotation frequency. In other words a normalized frequency of m in the following analysis is equivalent to m times the spindle frequency.

3-1. Transformation of Elemental Cutting Force Functions

The Laplace transforms of $p_x(\theta)$ and $p_y(\theta)$ in equation (12) are

$$\begin{bmatrix} P_x(s) \\ P_y(s) \end{bmatrix} = \begin{bmatrix} 1 & K_r \\ -K_r & 1 \end{bmatrix} \begin{bmatrix} P_1(s) \\ P_2(s) \end{bmatrix} \tag{20}$$

The Laplace transform of $p_1(\theta)$ can be derived from equation (13) using the complex convolution theorem:

$$P_1(s) = \frac{1}{4\pi j} \int_{q_0-j\infty}^{q_0+j\infty} \frac{2}{q^2+4} W(s-q)\, dq \qquad q_0 > 0 \tag{21}$$

where

$$W(s) = \frac{e^{-s\theta_1} - e^{-s\theta_2}}{s} \tag{22}$$

which is the Laplace transform of $w(\theta)$. By Cauchy's residue theorem, $P_1(s)$ can be shown to be

$$P_1(s) = \frac{1}{2(s^2+4)} \left[e^{-s\theta_1} (s \sin 2\theta_1 + 2\cos 2\theta_1) - e^{-s\theta_2} (s \sin 2\theta_2 + 2\cos 2\theta_2) \right] \tag{23}$$

Similarly, $P_2(s)$ can be shown as

$$P_2(s) = \frac{e^{-s\theta_1} - e^{-s\theta_2}}{2\,s} - \frac{1}{2(s^2+4)}\left[e^{-s\theta_1}\,(s\cos 2\theta_1 - 2\sin 2\theta_1) - e^{-s\theta_2}\,(s\cos 2\theta_2 - 2\sin 2\theta_2)\right] \qquad (24)$$

The Fourier transform can be obtained by substituting $s=j\omega$ into the above equations since $j\omega$ axis is in the region of convergence of $P_1(s)$ and $P_2(s)$. The frequency spectrum of the elemental cutting forces are shown in Figure 7 for various cutting conditions. It is seen in the figures that the position of the workpiece relative to the cutter has significant effects on the dynamics of the cutting force system, especially when the radial depth of cut is small.

3-2 Transform of Chip Width Density Function

The Fourier transforms of chip width density function $cwd(\theta)$ can be derived from Figure 4:

$$CWD(\omega) = \frac{2R}{\tan\alpha}\,\frac{\sin\frac{\omega\theta_a}{2}}{\omega}\,e^{-j\omega\frac{\theta_a}{2}} \qquad (25)$$

The Fourier transform assumes the form of a sinc function, which has periodic zeros with a period of $2\pi/\theta_a$. Figure 8 illustrates the effects of tool-workpiece geometry on the frequency spectrum of the chip width density function. It is evident from the figure that the axial depth of cut significantly affects the DC content of the spectrum, while the cutter radius and helix angle dominate the zeros of the spectrum.

3-3. Transform of Tooth Sequence Function

The Fourier transform of the tooth sequence function can be shown from equation (17):

$$TS(\omega) = t_x\,n\sum_{k=-\infty}^{\infty}\delta(\omega - nk) \qquad (26)$$

Since $ts(\theta)$ is a periodic impulse sequence function in the angular domain, its Fourier transform is also a periodic discrete impulse function with a period of n. This implies that the cutting forces have non-zero frequency contents only at the harmonics of the tooth passing frequency in addition to their DC components.

3-4. Transform of the Total Cutting Forces

The Fourier transform of the total cutting force is the product of the transforms of the elemental cutting force function, the chip width density function, the tooth sequence function, and the tangential specific cutting pressure constant. That is

$$\begin{bmatrix} \bar{F}_x(\omega) \\ \bar{F}_y(\omega) \end{bmatrix} = \begin{bmatrix} 1 & K_r \\ -K_r & 1 \end{bmatrix}\begin{bmatrix} P_1(\omega) \\ P_2(\omega) \end{bmatrix} . CWD(\omega) . TS(\omega) . K_t \qquad (27)$$

The total cutting force in the angular domain is represented by equation (20) in a convolution integral framework. As an alternative, they can now be expressed in a more useful form using Fourier integral formula:

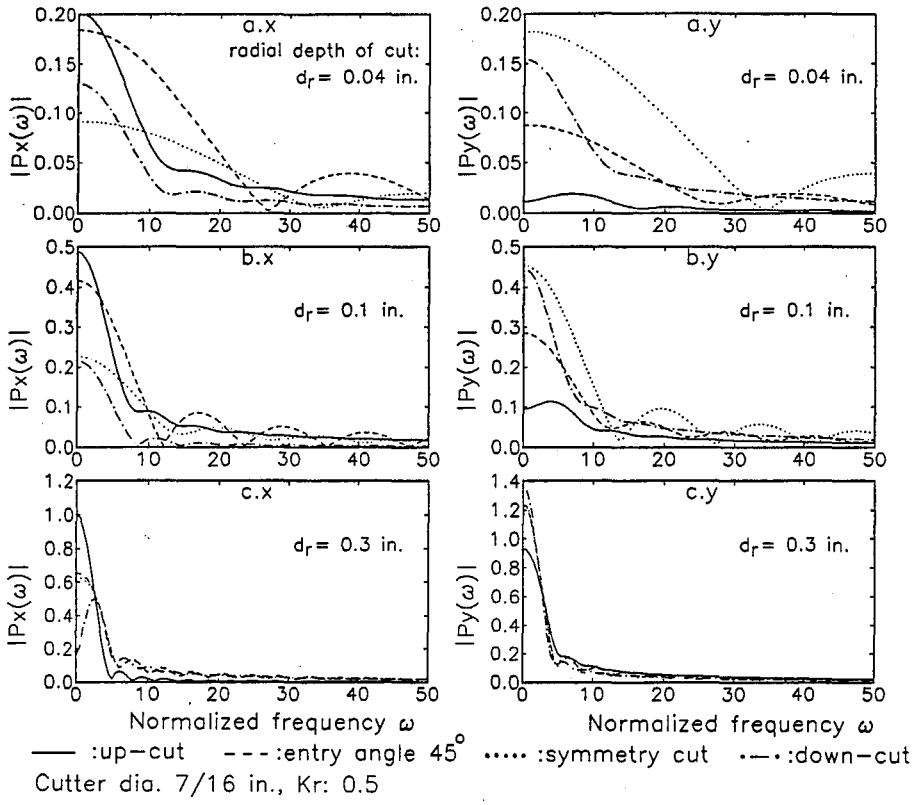

Figure 7. Frequency spectra of elementary cutting forces for various cutting geometry.

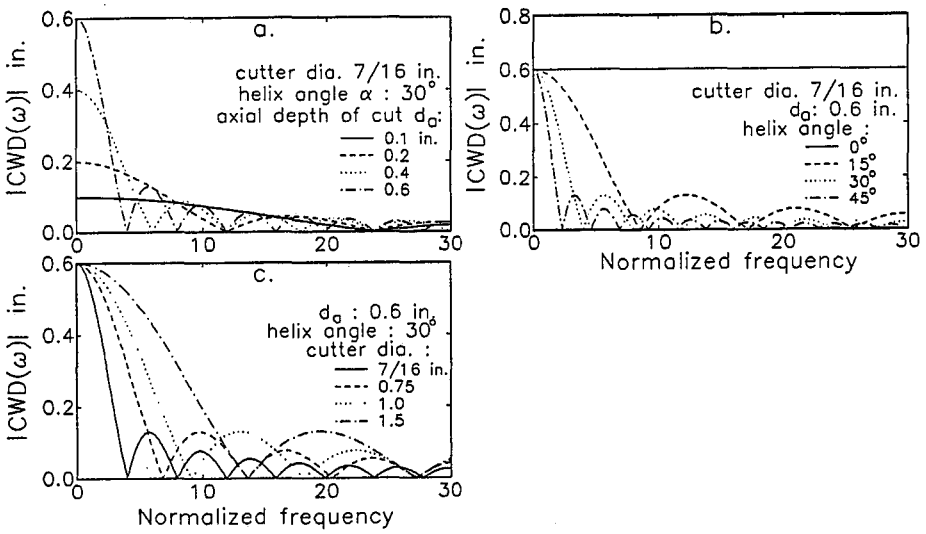

Figure 8. Spectra of chip width density function CWD(ω) for various cutter geometry.

$$\begin{bmatrix} \bar{f}_x(\theta) \\ \bar{f}_y(\theta) \end{bmatrix} = \frac{K_t t_x}{2\pi} \int_{-}^{} TS(\omega)\, CWD(\omega) \begin{bmatrix} 1 & K_r \\ -K_r & 1 \end{bmatrix} \begin{bmatrix} P_1(\omega) \\ P_2(\omega) \end{bmatrix} e^{j\omega\theta}\, d\omega$$

$$= \frac{K_t t_x}{2\pi} \int_{-}^{} n \sum_{k=-\infty}^{\infty} \delta(\omega - nk)\, CWD(\omega) \begin{bmatrix} P_x(\omega) \\ P_y(\omega) \end{bmatrix} e^{j\omega\theta}\, d\omega$$

$$= \sum_{k=-\infty}^{\infty} \begin{bmatrix} A_{xk} \\ A_{yk} \end{bmatrix} e^{jnk\theta} \tag{28}$$

where

$$\begin{bmatrix} A_{xk} \\ A_{yk} \end{bmatrix} = \frac{n\, K_t t_x}{2\pi} CWD(nk) \begin{bmatrix} P_x(nk) \\ P_y(nk) \end{bmatrix} \tag{29}$$

It is noted from equation (28) that A_{xk}'s and A_{yk}'s are the coefficients of the Fourier series expansion of total cutting forces $\bar{f}_x(\theta)$ and $\bar{f}_y(\theta)$.

The total cutting force frequency spectrum is calculated based on equation (29) for three cutting cases each with different axial depths of cut as illustrated in Figure 9. The last case shown in the figure was calculated with a cutter engagement angle θ_a being equivalent to tooth passing angle θ_p. In this particular case a constant cutting force without any dynamic frequency component results, which coincides with the implications from convolution modelling as discussed in section 2-4.

The contribution of tooth sequence function, ts(θ), and chip width density function to the frequency spectrum of total cutting forces can be realized from equation (28). The tooth sequence function determines the frequencies at which dynamic components of the cutting forces will be present. Chip width density function possesses zeros, whose periodicity is a function of θ_a. Thus, it is possible to have a pair of TS(ω) and CWD(ω) such that the dynamic components of cutting forces do not exist regardless of other cutting parameters, in particular the parameters related to the elemental cutting force functions. Figure 9(c) is a depiction of such a cutting process.

On the other hand, tooth sequence function has no bearing on the DC component of cutting forces provided that the feed per tooth is constant. Chip width density contributes to the DC component through a gain of d_a, regardless of the helix angle and the cutter radius.

The effects of P_x and P_y on the force frequency spectrum are more complicated. The position and width of the window function w(θ), defined by the radial depth of cut and cutter radius, affects subtly the spectrum of these two elemental cutting forces. It can be shown that if the cutting window is located such that the elemental force has a symmetric shape, its spectrum will have clearly defined peaks and valleys and a high DC content similar to the frequency response of a low pass filter. If the elemental force has an anti-symmetric shape, its spectrum will have a low DC component and higher dynamic contents similar to a high pass filter response. These statements are evidenced by the spectrum shown in Figure 7.

The effects of elemental cutting forces on the total cutting forces DC component hinge upon the location and width of the cutting window, which is determined by the radial depth of cut, cutter radius and relative position of cutter and workpiece.

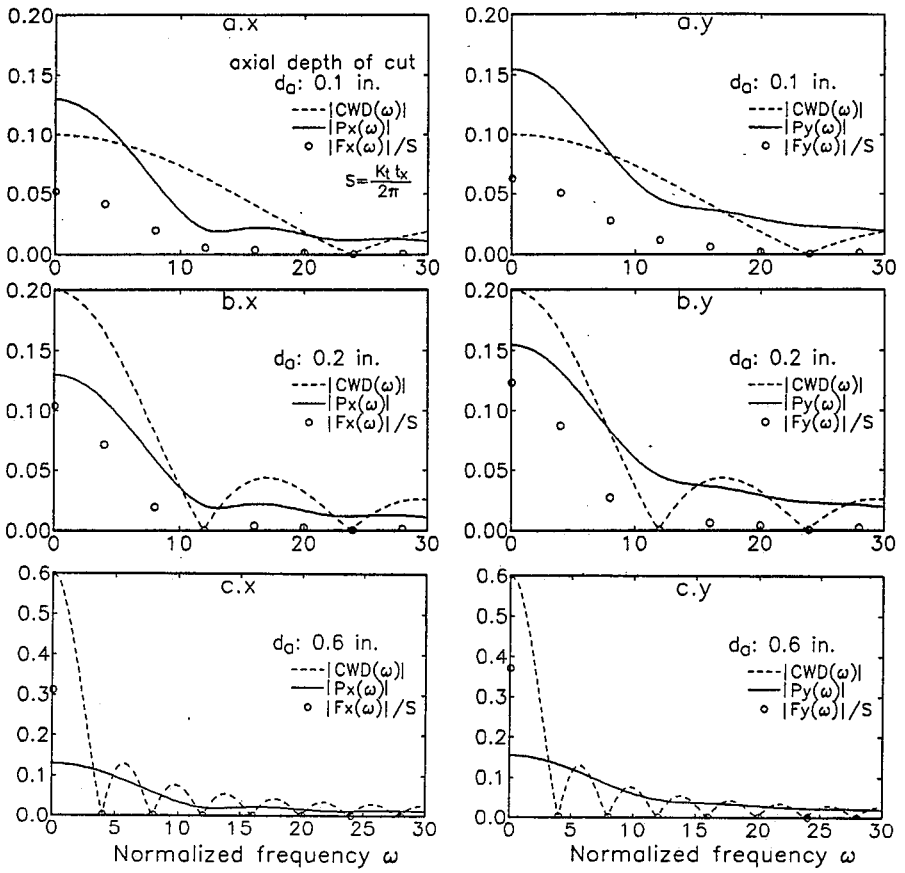

Figure 9. Frequency spectra of the total cutting forces $F_i(\omega)=K_t*TS(\omega)*CWD(\omega)*P_i(\omega)$. Circles represent the areas of the spectral impulses. Assumed cutting conditions are: cutter dia.=7/16 in., helix angle=30°, flute number=4, K_r=0.5, d_t=0.04 in., down-cut.

4. Experimental Verification

A series of end milling experiments was conducted to evaluate the validity of the analytical frequency domain model. The experimental cutting parameters were identical to those used in the three calculation cases shown in Figure 9. Cutting was performed with Aluminum 2024-T4 on a vertical milling machine running at 297rpm and 0.00675inch feed per tooth. The data acquisition system consisted of a two-component dynamometer, signal conditioning unit and a two channel PC-based digitizer with a sampling rate of 1KHz. Digitized cutting force data are transformed into frequency domain using standard FFT software. Since the cutting forces are inherently periodic due to the spindle rotation, the frequency spectrum obtained is discrete with a fundamental frequency equivalent to the spindle frequency. The spectral density function associated with the discrete frequencies are the same as the coefficients in the Fourier series representation of the digitized cutting force data.

Due to the lack of cutting pressure constants K_t and K_r for the specific work material and cutting conditions, a similar approach to that of Kline et al. [1983] was used to obtain these two constants from the x and y DC components of the experimental cutting force data. It can be shown from equation (28) that

Table 1. K_t and K_r calculated from average cutting forces

Cases	d_a (inch)	K_t(lbf/in^2)	K_r
a	0.1	246000	0.593
b.	0.2	240990	0.741
c.	0.6	218070	0.593

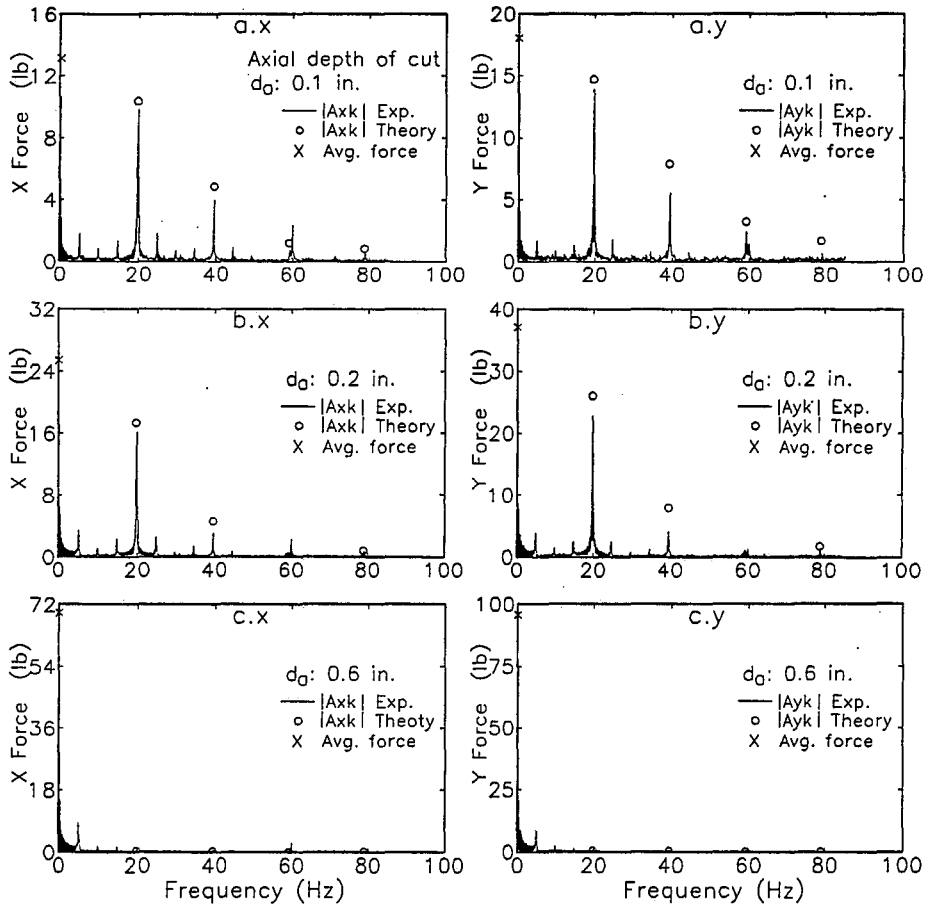

Figure 10. Comparison between the analytically calculated cutting force coefficients and experimental results. Workpiece material was aluminum 2024-T4 and spindle speed was 297 rpm. Other cutting conditions were identical to those of Figure 9 (cutter dia.=7/16 in., helix angle=30°, flute number=4, d_r=0.04 in., down-cut) except that K_t and K_r in Table 1 were used for the calculation of analytical cutting forces.

$$\begin{bmatrix} K_t \\ K_t K_r \end{bmatrix} = \begin{bmatrix} P_1(0) & P_2(0) \\ P_2(0) & -P_1(0) \end{bmatrix}^{-1} \begin{bmatrix} A_{x0} \\ A_{y0} \end{bmatrix} \left[CWD(0) \frac{n\, t_x}{2\pi} \right]^{-1} \tag{30}$$

in which A_{x0} and A_{y0} are the DC components of the measured forces. Constants K_t and K_r calculated in three different cutting conditions are listed in Table 1.

The model-predicted Fourier series coefficients were calculated by substituting K_t and K_r in equations (28) and (29) with the experimentally obtained values. Note that the frequency domain model, (28) and (29), is used herein to estimate the dynamic characteristics of cutting forces based upon given specific cutting pressures. To evaluate the validate of the proposed model, Fourier series coefficients from measurements and those from the model are compared at the first harmonic, the second harmonic, and the third harmonic of the tooth passing frequency (20 Hz) as shown in Figure 10. The experimental spectra at 60 Hz have lost their fidelity due to in-line electrical disturbances. It is seen from the figures that the results from experiments agree well with that from the analytical model in general. Notice that spectrum peaks occur at spindle frequency and at the sidebands of the harmonics frequencies, besides, the model-calculated Fourier coefficients are consistently higher than their experimental counterparts. This point is consistent with the observation reported by Kline [1983] regarding the effects of cutter runout on the frequency contents. He noted that the frequency content at the tooth passing frequency is shifted to the spindle frequency in the presence of cutter runout.

5. Summary

A closed form expression for the cutting forces in end milling was derived as explicit functions of cutting conditions and tool/workpiece geometry. This was achieved by decomposing the cutting process into three uncorrelated component functions, namely the elemental cutting force function, the chip width density function, and the tooth sequence function. The total cutting forces were derived as the angular convolutions of these three component functions. The effects of various cutting parameters on the cutting forces were discussed and illustrated in the context of the convolution model.

The analysis was extended into the Fourier domain by taking the frequency multiplication of the transforms of the three component functions. Fourier series coefficients of the cutting forces are shown to be algebraic functions of various tool parameters and cutting conditions. The illustration of the cutting force mode shapes in relation to the milling process conditions was discussed based on simulation results, which are presented in terms of the power spectra of the cutting component functions as well as that of the total cutting forces in both x and y directions.

A series of end milling experiments were performed to validate the analytical model. The discrete spectral density function of the measured forces agreed well with the calculated Fourier series coefficients at the harmonics of the tooth passing frequencies for different axial depths of cut. The frequency shift in the force spectrum from tooth passing frequency to spindle rotation frequency as a result of cutter runout was also observed.

References

Armarego, E. J. A., and Despande, N. P., "Computerized Predictive Cutting Model for Forces in End-Milling Including Eccentricity Effects," Annals of the CIRP, Vol. 38, pp. 45-49, 1989.

Ber, A., Rotberg, J. and Zombach, S., "A Method for Cutting Force Evaluation of End Mills," Annals of the CIRP, Vol. 37, pp. 37-40, 1988.

Fu, H. J., DeVor, R. E., and Kapoor, S. G., "A Mechanistic Model for the Prediction of the Force System in Face Milling Operations," ASME J. of Engineering for Industry, Vol. 106, pp. 81-88, Feb. 1984.

Fussel, B. K. and Srinivasan, K., "On-line Identification of End Milling Process Parameters," Proceedings of the USA-Japan Symposium on Flexible Manufacturing, Minnesota, pp. 967-974, 1988.

Gygax, P. E., "Dynamics of Single-Tooth Milling," Annals of the CIRP, Vol. 28, pp. 65-70, 1979.

Gygax, P. E., "Experimental Full Cut Milling Dynamics," Annals of the CIRP, Vol. 29, p.p. 61-66, 1980.

Kline, W. A., DeVor, R. E., Lindberg, J. R., "The Prediction of Cutting Forces in End Milling with Application to Cornering Cut," International Journal of Machine Tool Design and Research, Vol. 22, pp. 7-22, 1982.

Kline, W. A. and DeVor, R. E., "The Effect of Runout on Cutting Geometry and Forces in End Milling," International Journal of Machine Tool Design and Research, Vol. 23, No 2/3, pp. 123-140, 1983.

Koenigsberger, F., and Sabberwal, A. J. P., "An Investigation into the Cutting Force Pulsations During Milling Operations," International Journal of Machine Tool Design and Research, Vol. 1, pp. 15-33, 1961.

Lauderbaugh, L. K., and Ulsoy, A. G., "Dynamic Modeling for Control of the Milling Process," ASME J. of Engineering for Industry, Vol. 111, pp. 367-374, November 1988.

Martellotti, M. E., "An Analysis of the Milling Process," Transaction of. ASME, Vol. 63, pp. 677-700, 1941.

Martellotti, M. E., "An Analysis of the Milling Process, Part 2: Down Milling," Transaction of ASME, Vol. 67, pp. 233-251, 1945.

Rohrs, C., Valavani, L., Sthans, M., and Stein, G., "Robustness of Continuous-time Adaptive Control Algorithms in the Presence of Unmodelled Dynamics," IEEE Transaction on Automatic Control, Vol. 30, pp. 881-889, 1985.

Sabberwal, A. J. P., presented by F. Koenigsberger, "Chip Section and Cutting Force During the Milling Operation," Annals of the CIRP, 10, pp. 197-203, 1961/62.

Sutherland, J. W., and DeVor, R. E., "An Improved Method for Cutting Force and Surface Error Prediction in Flexible End Milling Systems," ASME J. of Engineering for Industry, Vol. 108, pp. 269-279, Nov. 1986.

Tlusty, J., and MacNeil, P., "Dynamics of Cutting Forces in End Milling," Annals of the CIRP, Vol. 24, pp. 21-25, 1975.

Tomizuka, M., Oh, J. H., and Dornfeld, D. A., "Model Reference Adaptive Control of the Milling Process," Proceedings of the Symposium on Control of Manufacturing Processes and Robotic Systems, D. Hardt ed., ASME Winter Annual Meeting, pp. 56-63, 1983.

Zhou, R., and Wang, K. K., "Modelling of Cutting Force Pulsation in Face-Milling," Annals of the CIRP, Vol. 32, pp. 21-26, 1983.